Nutrient-imbalanced Conditions Shift the Interplay Between Zooplankton and Gut Microbiota

Yingdong Li
Hong Kong University of Science and Technology https://orcid.org/0000-0002-4971-4165
Zhimeng Xu
Hong Kong University of Science and Technology
Hongbin Liu (liuhb@ust.hk)
Department of Ocean Science, The Hong Kong University of Science and Technology, Clear Water Bay, Kowloon, Hong Kong SAR, China https://orcid.org/0000-0002-3184-2898

Research article

Keywords: Metatranscriptomic analysis, Zooplankton, Daphnia magna, Gut microbe, stoichiometric homeostasis

Posted Date: July 22nd, 2020

DOI: https://doi.org/10.21203/rs.3.rs-43571/v1

Version of Record: A version of this preprint was published on January 7th, 2021. See the published version at https://doi.org/10.1186/s12864-020-07333-z.

Abstract

Nutrient stoichiometry of phytoplankton changes frequently with aquatic ambient nutrient concentrations, which is mainly influenced by environmental factors and the dynamics of ecosystems. Consequently, the stoichiometry of phytoplankton can markedly alter the metabolism and growth of zooplankton. However, the effects of nutrient-imbalanced prey on the interplay between zooplankton and their gut microbiota remain unknown. Using metatranscriptome sequencing, neutral community model (NCM), and experimental validation, we investigated the interactions between *Daphnia magna* and its gut microbiota on nutrient-imbalanced algal diet. Our results showed that in nutrient depleted water, nutrient-enriched zooplankton gut stimulated the accumulation of microbial polyphosphate and the assimilation of ammonia under phosphorus and nitrogen limited diet, respectively. Comparing with nutrient replete group, both N and P limitation had markedly promoted the gene expression of gut microbial for organic matter degradation but repressed that for anaerobic metabolisms. Besides, with N and P limited diet, the gut microbial community exhibited a higher fitting to NCM, suggesting increased ambient-gut exchange process favored by compensatory feeding of *D. magna*. This process also elevated oxygen level in the gut and explained the repressed anaerobic metabolism of gut microbes. Further axenic grazing experiment revealed that bacteria can still benefit *D. magna* to achieve a better growth under nutrient-imbalanced diet by enhancing their digestion capability. Together, these results demonstrated that under nutrient-imbalanced diet, the microbes not only benefit themself by absorbing excess nutrients inside zooplankton gut but also benefit zooplankton to achieve a better adaptation.

Introduction

The concept of stoichiometric homeostasis is the ability of an organism to maintain its elemental or biochemical composition, despite changes in the quality of resource supply (i.e., food quality) (Sterner and Elser 2002, Hessen et al. 2004). In aquatic systems, primary producers usually experience dynamic fluctuations in the availability of nutrient resources. For example, For example, due to the influence of Asia Monsoon, the seasonal cycle of freshwater discharge and the hydrodynamics mixing of different water masses, phytoplankton in the Pearl River estuary experience fluctuation between P and N limitation (Xu et al. 2008). In general, phytoplankton are more flexible in regulating their elemental composition (e.g., C:P, C:N, and N:P ratios) than most heterotrophs (Glibert et al. 2011, Golz et al. 2015).

In the framework of stoichiometry, prey with a similar elemental ratio as their consumers can enhance the assimilation efficiency of the consumers (Sterner and Elser 2002). However, the highly variable stoichiometry of aquatic primary producers means that herbivorous zooplankton will face the problem of nutritional imbalance frequently (Sterner et al. 1998). A large number of studies have been conducted to investigate the effects of nutritionally imbalanced algal food on crustacean mesozooplankton (Boersma 2000, Boersma et al. 2008). Results of these studies indicate that the elemental composition of primary producers not only affects the growth, grazing behavior, and fecal parameters of herbivorous zooplankton, but it also constrains ecological processes, such as food-web dynamics and the composition of fecal pellets, which are key for nutrient recycling (Elser and Urabe 1999, Glibert et al.

2011). However, little is known about the effects of the nutrient-imbalanced algal prey on the metabolic interactions between zooplankton and their gut microbes, as well as the properties of the fecal pellets produced by the zooplankton.

The physiological changes that occur in zooplankton have dramatic effects on global primary production and the nutrient cycle, as well as the overall fitness and dynamics of the oceanic ecosystems (Prahl and Carpenter 1979). Recent studies have revealed that gut microbiota are essential for the survival and environmental adaption of herbivorous zooplankton under various conditions (Macke et al. 2017a, Callens et al. 2018). Indeed, the gut microbiota influences nutrient uptake efficiency (Chevalier et al. 2015), essential amino acids supply (Leitão-Gonçalves et al. 2017), food digestion rate (Brune and Dietrich 2015), detoxification of toxic substances (Macke et al. 2017a), resistance to pathogenic infection (Foster and Neufeld 2013), and the growth of the host (Foster and Neufeld 2013, Callens et al. 2018). In addition, the composition and metabolic function of the gut microbiota of zooplankton are highly dependent on the ingested ambient bacteria such that although some will be excreted, others will remain and survive (Tang et al. 2010). However, it remains unclear how the ingested bacteria react to the transformation in their environment, from the oligotrophic ambient water to the eutrophic zooplankton gut, as the amassed food particles in the latter create a nutrient-rich environment. It is therefore important to investigate how zooplankton benefit from the change of metabolic activity of its intestinal microbiota under a nitrogen- or phosphorus-deficient algal diet.

There are currently few reports describing how gut microbiome might affect the biochemical properties of zooplankton fecal pellets, which are one of the main sources of particulate organic carbon that can be utilized by microorganisms in the water column or exported to the deep ocean (Carlson and Hansell 2015, Steinberg and Landry 2017). The physical and chemical properties (e.g., the density and organic content) of fecal pellets are strongly influenced by the type, quality, and quantity of the prey and its associated microbes. It is therefore reasonable to hypothesize that microbial metabolism in the zooplankton gut plays an important role in mediating the digestibility of the prey and the biodegradability of the fecal pellets, hence affects the carbon and nutrient recycling and flux in aquatic ecosystems. In the present study, we sequenced the metatranscriptome of the gut extracted from the model zooplankton organism, *Daphnia magna*, after they were fed with different types of nutrient-imbalanced algal prey. In this investigation, we aimed to decipher the interdependence and interplay between the host and gut microbiota on a nutrient-imbalanced algal diet. To achieve that, we investigated how microbiota, which were previously subjected to nutrient starvation stress, reacted to the nutrient-enriched *D. magna* intestinal environment; how the host and gut microbiota cooperated in the provision of nutrients; and how the gut microbiota mediated the properties of the fecal pellets of *D. magna* on a nutrient-imbalanced algal diet.

Methods

Preparation of the experimental organisms

The algal prey, *Chlamydomonas reinhardtii* (CC1690), was grown in liquid BG11 medium (Rippka et al. 1979), and *D. magna* was cultured in ADaM medium (Klüttgen et al. 1994). Both were cultured in a sterile temperature-controlled chamber at 23 ± 1 °C on a 14:10 h light/dark cycle under 20 μmol m^{-2} s^{-1} illumination, with constant stirring and aeration. *D. magna* were kept at a density of one individual per 10 mL and fed with saturating amounts of *C. reinhardtii* (10^5 cells/mL) each day, and the medium was refreshed once a week. N- and P-limited *C. reinhardtii* cultures were prepared with liquid nitrogen and phosphate-free BG11 medium (Rippka et al. 1979), respectively.

Grazing Experiment

Three different *C. reinhardtii* cultures (cultures grown in nutrient-balanced, N-limited or P-limited media) were used to feed the *D. magna* for seven days (Fig. 1). The prey was centrifuged and re-suspended with an appropriate amount of *D. magna* culture medium before being fed to the *D. magna*. All three experimental groups were constructed in triplicate in 1 L PC bottles and incubated in the sterile temperature-controlled chamber mentioned above. The *D. magna* were kept at a density of one individual per 10 mL and they were fed with saturating amounts of nutrient-balanced, N-limited, or P-limited *C. reinhardtii* cells (10^5 cells/mL), each day. For measuring the clearance and ingestion rates, triplicate 150 mL PC bottles were prepared for the three experimental groups (nutrient-balanced, N-limited, and P-limited), and the medium and bottles were renewed every day to avoid the influence of any remaining algae in the bottles. In addition, in these experiments the newly born neonates were removed from the culture and counted. To avoid cell aggregation or settlement, the cultures were gently agitated manually 2 to 3 times a day. As a control for the grazing experimental groups and to calculate the ingestion rate, another three groups were prepared in triplicate using the same concentration and type of *C. reinhardtii* but no *D. magna*. The calculation of ingestion and clearance rate was based on the previous reported method (Zhang et al. 2017).

Flow Cytometry Analysis

To determine the bacterial cell abundance inside the liquid algal cultures, filtrate were collected from the three different experimental groups before and after the grazing experiment via filtration through a 1 μm-pore-size filter. The filtrate were then stained with SYBR Green I solution at a ratio of 10:1 (the SYBR Green I solution was 1:1000 diluted with Milli-Q water; Molecular Probes) and incubated at 37°C in the dark for 1 h (Marie et al. 1997). The bacterial cell abundance was then examined using the Becton-Dickson FACSCalibur flow cytometer described above (details are provided in the Supporting Information).

Construction Of The Axenic Culture

In one series of experiments, *C. reinhardtii* and *D. magna* were separately made into sterile cultures, using antibiotics, as described in previous studies (Kan and Pan 2010, Macke et al. 2017b). For the sterile *C.*

reinhardtii culture, R medium containing a cocktail of antibiotics (ampicillin, carbendazim, and cefotaxime (Sigma, Germany)) was used to obtain pure *C. reinhardtii* colony. The ampicillin and cefotaxime were used at final concentrations of 500 µg/mL and 100 µg/mL, respectively. As these antibiotics can be heat-inactivated, they were added to the agar medium after it was autoclaved and immediately prior to pouring the plates. In contrast, carbendazim is heat stable but only barely soluble, and so this was added to the agar medium (to a final concentration of 40 µg/mL) before it was autoclaved and then the solution was mixed well before the plates were poured (Kan and Pan 2010). After 14 days cultivation of plates in the sterile temperature-controlled chamber, the pure algal colonies in the antibiotics-containing agar plates were then inoculated into autoclaved liquid BG11 medium and the existing of bacteria was examined with a Becton-Dickson FACSCalibur flow cytometer. The level of microbial contamination was also examined at the end of the feeding experiment.

Bacteria-free eggs were obtained by disinfecting eggs, from the normally fed *D. magna*, through exposing them to 0.25% ampicillin (Sigma, Germany) for 30 min. Part of the antibiotic-treated eggs was crushed with a pestle and filtered through a 0.22 µm membrane for PCR assessment of remaining bacteria (Li et al. 2019b). After rinsing with sterile ADaM to remove ampicillin, the eggs were transferred to a sterile six-well plate for hatching. The axenic grazing experiment was conducted, where the axenic *C. reinhardtii* was used as prey. At the end of the grazing experiment, all the *D. magna* (thirty individuals in total) in each experimental group (Normal, N-limited, P-limited, Germ-free Normal, Germ-free N-limited, and Germ-free P-limited) were used for the measurement of body length.

Nutrient Analyses

Before the beginning of the grazing experiment, samples of *C. reinhardtii* that had been grown in the different conditions were collected for the analysis of cellular carbon, nitrogen, and phosphorus. Samples were taken from the respective culture bottles by filtering 15 to 25 mL of each culture onto pre-combusted (i.e., at 550°C for 5 h) GF/C glass-fiber filters. After the seven-day grazing experiment or following 6-h starvation, one *D. magna* from each experimental group was transferred to a pre-combusted 25 µm GF/C filter for determination of elemental composition (C and N), and another *D. magna* of similar body length and weight as the first, was collected for the phosphorus measurement. Cellular carbon and nitrogen in both the *D. magna* and *C. reinhardtii* were measured with a CHNS (carbon, hydrogen, nitrogen, sulphur) elemental analyzer (FlashSmart CHNS, Thermo Scientific Inc. Massachusetts, USA) according to previously described protocol (Zhang et al. 2015). The amount of phosphorus (in the form of orthophosphate) was analyzed manually following acidic oxidative hydrolysis with 1% HCl (Grasshoff et al. 2009) using a spectrophotometer at a wavelength of 880 nm, with a detection limit of 0.5 µmol/L.

Gut extraction of D. magna

For the purpose of molecular investigation, triplicate 1 L PC bottles were prepared for the three experimental groups (nutrient-balanced, N-limited, and P-limited) with 80 individuals raised in each bottle. At the end of the seven-day grazing experiment, the gut of all *D. magna* was extracted with sterilized (i.e.,

autoclaved and 70% ethanol steeped) dissection tweezers (Regine 5, Switzerland) in a sterile Petri dish under a stereomicroscope. Before each gut extraction procedure, tweezers were flame-sterilized and rinsed with 70% alcohol. Each of the extracted guts from the various experimental groups, was placed into a 1.5 mL sterile Eppendorf tube and dissociated into a cell suspension according to previous report (Li et al. 2019a). The cell suspension was then filtered through a 0.22 μm polycarbonate membrane (EMD Millipore, Billerica, MA, USA) with addition of 500 μL RNA protect reagent (Qiagen, Germany). In order to assess the potential operation contamination, the tweezers and Petri dishes used to prepare the cell suspension were rinsed with water and this was then filtered through another a 0.22 μm membrane for the detection of contamination. Therefore, a total of eighteen filters were used to collect the cell suspension from the gut and the contamination separately. All the filters were preserved in sterile 1.5 mL Eppendorf tubes and stored at -80 °C until RNA extraction.

Detection of microbial polyphosphate

Ten adult *D. magna* from each experimental group (i.e., nutrient-balanced, N-limited, or P-limited), were placed in 100 mL sterile ADaM medium to empty their gut, and their fecal pellets were collected by filtering the medium through a 2.0 μm polycarbonate membrane (EMD Millipore, Billerica, MA, USA). The membrane was sonicated for 30 s to release any bacteria that were attached to the fecal pellets into the suspension. The fecal detritus was removed via centrifugation at 4,000 g for 5 min, and the supernatant was used for the detection of microbial polyphosphate (polyP). To measure microbial polyP in zooplankton and alage cultures, the culture was firstly filtered through a 3 μm membrane to remove the alage and large particles. Then the filtrate was used for the detection of microbial polyP according to a previous report (Kulakova et al. 2011). In brief, the suspended bacterial cells (in a 96-well plate) were stained with 25 mM Tris/HCl at pH 7.0 containing 500 μg/mL DAPI for 10 min, and the level of fluorescence was measured using a Flex Station 3 multimode microplate reader with excitation and emission filters of 420 nm and 550 nm, respectively (Molecular Devices, Sunnyvale, CA, USA). The microbial protein was then further quantified as described previously (Binks et al. 1996), and the fluorescence intensity of microbial polyP was expressed as relative fluorescence units (r.f.u.) per mg of total cellular protein.

Dna Extraction And Pcr Amplification Of 16s Rrna Gene

The validation of bacterial contaminant and bacteria-free eggs was achieved through DNA extraction and PCR amplification of the 16S rRNA gene. Total genomic DNA was extracted from the filters of dissection tools rinse water, and from randomly sampled *D. magna* germ-free eggs, using a PureLink Genomic DNA kit (Invitrogen, ThermoFisher Scientific Corp., Carlsbad, CA, USA). Due to that failures of gut extraction happens occasionally, different number of *D. magna* guts were collected from normal (10), N-limitation (7) and P-limitation (12) experimental groups. Each of these guts was placed into tubes individually for amplification of the 16 s rRNA gene. The extracted DNA was then eluted into 100 μl Tris-EDTA (TE) buffer

for PCR amplification. These 29 gut microbial communities were amplified and sequenced as described previously (Liu et al. 2017).

Analysis Of 16s Rrna Gene

The sequenced contig reads between 135 and 152 bp were preserved, and primers as well as low-quality reads were removed with FASTX-Toolkit (Pearson et al. 1997). Reads with an average Phred score < 25 were discarded, as were reads with any consecutive runs of low-quality bases > 3. The lowest quality score allowed was 3, the minimum of continuous high-quality bases was 75% of whole read length, and the maximum number of ambiguous bases was 0 (Pan et al. 2019). Chimeras were identified and removed using UCHIME (Edgar et al. 2011). The remaining high-quality sequences were merged according to the experimental treatments, and the taxonomically assignment was processed with Silva database (version 123) by following the previous reported method (Li et al. 2018). Finally, sequences were clustered into OTUs with a 97% sequence similarity cutoff. To get overall gut community distribution pattern within each experimental treatment, the OTUs were normalized with the sample number prior to further analyses. The results were further used in a Lda (linear discriminant analysis) effective size (LEfSe) analysis, which is typically used to reveal the taxonomic differences between experimental groups.

Rna Isolation And Metatranscriptomic Sequencing

The filters collected during the various experiments were briefly thawed on ice and the RNA protection solution was removed as previously described (Xu et al. 2013). In brief, the filters were transferred to a new 0.7-ml tube with a pinhole in the bottom. This was placed on top of a 1.5-ml centrifuge tube, and the residual RNA protection reagent was removed from the filters when the two tubes were centrifuged at 1000 rpm for one min. RNA extraction was achieved with the Totally RNA isolation kit (Ambion Inc, Germany) according to the manufacturer's protocol. The Turbo DNA-free DNase kit (Ambion Inc, Germany) was used to remove the remaining DNA, and the MicroPoly (A) Purist kit (Ambion Inc, Germany) was used to isolate mRNA; both of these kits were used according to the manufacturer's instructions. A Nanodrop spectrophotometer (Nanodrop Technologies, Wilmington, USA) was used to examine the purity of the extracted RNA, and the RNA BR Assay kit (Life Technologies, Invitrogen, Germany) in conjunction with a Qubit® 2.0 flurometer was utilized to estimate the concentration. A Ribo-Zero Magnetic kit (Epicentre, Madison, WI) was used to remove any remaining ribosomal RNA, after which the TruSeq mRNA Library Preparation kit (San Diego, CA, USA) was used to construct the Illumina sequence library. The pooled mRNA from each triplicate were barcoded and sequenced with an Illumina HiSeq2500 sequencer (Novogene Co., Ltd., China), generating between 131.3 and 207.1 million 150 bp paired-end reads per replicate.

Disentangling Partner Reads From The Holobiont System

According to the barcode, the sequencing data were assigned to nine experimental groups (Normal, N-limitation and P-limitation). The quality control of sequenced reads was performed as described in previous reports (Gong et al. 2018, Li et al. 2018). In addition, the reads that belong to different parts of the holobiont (i.e., *D. magna* and its gut microbiota), were separated by applying a previously reported method (Meng et al. 2018). In brief, the genome and previously published RNA-seq datasets of *D. magna* (Orsini et al. 2016) were downloaded to a local server to construct a host reference library, and the bacterial fractions of the Tara Oceans meta-genomic gene catalogue (OM-RGC) and non-redundant (nr) database were extracted with the blastdbcmd program (Camacho et al. 2009) to build a microbiota reference library. The SRC_c software (Marchet et al. 2018) was then used to map the metatranscriptomic data either to the host or to the gut microbiota with indexed k-mers set to 32 and suggested default similarity s value (50%).

Reads Assembly And Downstream Analysis

After separation of the metatranscriptomic data, the reads were assembled into longer transcripts, separately, using Trans-ABySS v2.0.1 (Robertson et al. 2010) with multiple k-mer sizes from 32 to 92, and a step of 4. Transdecoder (v5.3.0) (Haas et al. 2013) was used to predict the open reading frames (ORFs) of the assembly result. The annotation of ORFs was achieved using DIAMOND (v0.9.21.122) (Buchfink et al. 2015) against the Kyoto Encyclopedia of Genes and Genomes (KEGG) database and the nr database, with the following parameters: blastp; k parameter = 1 ; and an e-value = 10^{-7}. For calculation of the coverage information of ORFs, reads were mapped back to the ORFs using Bowtie 2.2.9 (Langmead and Salzberg 2012) and SAMtools v1.9 (Li et al. 2009). The differentially expressed genes (DEGs) between experimental groups were calculated according to a previous report (Li et al. 2019a), using the edgeR package in R (Robinson et al. 2010). The DEGs were defined with the criteria of $|\log_2 (\text{fold change})| > 1$ and p-value < 0.05 shown in the comparisons between experimental groups. In addition, the genes encoding microbial butyrate synthesis were also identified using the specific database (Vital et al. 2014).

Gene Expression Validation

For each sample, HiScript® III RT SuperMix for qPCR (+ gDNA wiper) (Vazyme Biotech, Nanjing, China), was used for the reverse transcription of extracted RNA (500 ng). No reverse transcription (RT) control was used in the qPCR experiment for the detection of the possible remaining DNA in the extracted RNA. After the synthesis of cDNA, 1 µL (nearly 50 ng) from each cDNA sample was used for qPCR with a Fast start Universal SYBR Green Master mix kit (Roche, Germany) in a LightCycler 384 device (Roche, Germany). The thermocycling conditions were as follows: an initial hold at 50℃ for 2 min and at 95℃ for 10 min followed by 45 cycles of 95℃ for 15 s and 60℃ for 1 min. All reactions were performed in triplicate. The relative amount of mRNA was determined using the $2^{-\Delta\Delta Ct}$ method, and the 16S rRNA gene was selected as a reference for normalization of the gut microbe genes. The primers used to target

specific genes in the gut microbiota and *D. magna* were as previously described (Li et al. 2019a) and they are listed in Table S1.

Statistical Analyses

For the ingestion rate, reproduction, and final body length, data were presented as the mean ± SD derived from the biological replicates. Student's *t*-tests (two-tailed) were conducted with significance levels of $p < 0.05$. Sloan's neutral community model (NCM) was constructed to evaluate the contribution of neutral processes in *D. magna*'s gut community structure (Sloan et al. 2006). R software was used to perform the analysis. In this analysis, Nm is an estimate of dispersal between communities while the R^2 determines the overall fit to the neutral community model (Chen et al. 2017). Canonical correspondence analysis (CCA) was performed using the PAST 3.0 software.

Results

Construction of axenic cultures

Axenic *C. reinhardtii* cells were obtained from agar plates containing an antibiotic cocktail comprising ampicillin (500 μg/mL), carbendazim (40 μg/mL), and cefotaxime (100 μg/mL). It was apparent that after 14 days in cultivation, the antibiotics markedly inhibited the growth of other microorganisms (Fig. S1B),including prokaryotes and fungus, when compared with the antibiotic-absent control group (Fig. S1A). After inoculation of the axenic *C. reinhardtii* cells from the agar plate to sterile liquid media, the bacterial abundance was measured before and after the grazing experiment by flow cytometry. The results showed that there was a little bacterial contamination in the liquid algal culture (Table S2), however, this low bacterial levels did not impact the results of feeding experiments significantly. The 16S amplicon results obtained for the antibiotic-treated eggs, and the extracted gut of *D. magna* after being fed with different types of sterile algal prey, showed that there was no PCR product band in the gel, which confirmed that the *D. magna* were successfully manipulated into axenic conditions. In addition, without intestinal bacteria the body length and survival rate of *D. magna* were both markedly lower than these parameters in the normal group, where intestinal bacteria existed, in all treatments. Furthermore, in the sterile P- and N-limited groups, these same life history traits were much lower than they were in the sterile normal group after seven days of feeding (Fig. S2A).

Elemental composition of C. reinhardtii **and** D. magna

Manipulation of nutrients in the media produced *C. reinhardtii* cells with different elemental compositions. The N- or P-limited medium resulted in significantly lower amounts of cellular N or P, respectively, when compared with their nutrient-balanced counterparts (Table 1). Accordingly, *C. reinhardtii* cells showed the highest molar C:N ratio when cultured in N-limited medium, whereas the highest molar C:P ratio was detected in cells cultured in P-limited medium (Table 1). As *C. reinhardtii* is a source of food for *D. magna*, the distinctively different nutritional quality of these preys markedly affects

the elemental composition of the predator. Thus, measurements of the elemental composition of the *D. magna* indicated that the highest molar C:N and C:P ratios were detected in the cultures fed with N- and P-limited prey, respectively, regardless of whether the experimental group was germ-free or not.

Table 1
Summary of elemental composition of *C. reinhardtii* and *D. magna*

Experimental groups	*C. reinhardtii*		*D. magna*	
	C:N	C:P	C:N	C:P
Normal	7.5 ± 0.2	65.0 ± 6.1	12.1 ± 1.0	19.1 ± 0.7
N-limitation	16.7 ± 0.1	74.3 ± 8.7	16.0 ± 1.4	20.9 ± 1.2
P-limitation	15.4 ± 0.3	467.7 ± 89.8	20.9 ± 1.2	22.3 ± 1.0
Normal Germ-free	6.7 ± 0.4	57.4 ± 5.8	15.1 ± 0.7	20.0 ± 0.8
N-limitation Germ-free	14.5 ± 0.5	67.1 ± 4.6	17.4 ± 1.1	21.1 ± 1.3
P-limitation Germ-free	13.7 ± 0.7	551.4 ± 71.4	21.1 ± 0.6	22.1 ± 0.8

Effects of low-quality prey on the life history traits of the *D. magna*

The life history traits of the *D. magna* were markedly affected by the nutritional quality of their prey (Fig. 2). For example, the ingestion and clearance rates of *D. magna* were found to increase in the poor-quality diet, when compared with the normal diet group (Fig. 2A, B, C). The results also showed that the ingestion and clearance rates of the *D. magna* continuously increased with the length of time they were fed on low-quality prey, although in the P-limited group, the rates plateaued at day six. In addition, the number of neonates (Fig. 2D) and body length (Fig. 2E) both decreased when the *D. magna* were fed on poor-quality prey, with more severe effects found in the P-limited diet.

Disentanglement Of The Partner Transcriptome In The Holobiont

After RNA extraction, as well as sequencing the crushed gut of *D. magna*, the successful achievement of contamination-free laboratory operations was confirmed by a lack of PCR product in the rinse water. Approximately 131 to 207 million 150 bp paired-end reads were generated across the 9 samples (Table S3). The results showed that after disentanglement of the metatranscriptomic data, the percentage of reads that affiliated to the *D. magna* (host) and gut microbes ranged from 76.92–85.03%, and from 7.19–35.37%, respectively, across all the samples (Table 2). The number of assembled contigs for the host ranged from 227,920 to 306,664, whereas that for the gut microbiota ranged from 26,418 to 47,344 across all the samples. In addition, the N50 of assembled contigs of the *D. magna* and bacteria ranged from 891 to 1,597 (Table S4). A principal component analysis (PCA) of the identified ORFs in *D. magna* and its gut microbiota indicated that the biological replicates of each experimental group were close, but

far from other experimental treatments, which verified significant metabolic difference between different treatments and good repeatability among triplicates (Fig. 3A, B).

Table 2
Results of sequence disentanglement

Samples	Assigned to host library	Assigned to bacterial library	Shared	Unassigned
Normal-1	78.22	13.37	1.64	6.77
Normal-2	76.92	11.14	1.52	11.09
Normal-3	81.28	9.31	1.74	7.34
N-limitation-1	78.33	10.47	1.75	9.45
N-limitation-2	80.48	9.35	2.10	8.07
N-limitation-3	82.36	7.19	1.96	8.49
P-limitation-1	85.03	6.19	1.68	7.10
P-limitation-2	84.16	6.34	2.21	7.29
P-limitation-3	82.29	6.95	2.44	8.32
All values are % reads from holobiont				

Effects of different types of prey on the gut microbiota community

Using the amplified and normalized 16 s rRNA gene, we identified the taxonomic composition of the gut microbiota. Our results showed that *Ruminococcaceae* (affiliated to the *Clostridia* class within the *Firmicutes* phylum) and *Xanthomonadaceae*, (affiliated to *Gammaproteobacteria* within the *proteobacteria*) were significantly enriched in the nutrient-balanced group with LDA scores of 5.76 and 5.43, when compared with the N- and P-limited groups, respectively. Also, *Streptococcaceae* were more abundant in the N- and P-limited groups, when compared with the nutrient-balanced group, and *Planctomycetaceae* were enriched in the N-limited group (Fig. 4).

The NCM successfully described the frequency distributions of the 29 gut microbial communities in normal (R^2 = 0.542, m = 0.017), N limited (R^2 = 0.624, m = 0.038), and P limited (R^2 = 0.781, m = 0.023, Fig. 5) diets. A higher R^2 value in NCM not only indicates the data are well fit to the model, but also suggests a higher importance of neutral process in shaping the community. The promoted dispersal/immigration rate, m value, in N and P limited conditions indicated that the community forms and develops through an enhanced immigration from ambient water to the gut. Our result confirmed that the processes of passive dispersal and ecological drift (neutral process) had an important impact on the distribution of gut microbial communities in all three experimental groups, and the N and P limited diets further increased the importance of immigration process in shaping *D. magna*'s gut microbial communities.

The Metabolic Variation Of Gut Microbiota Under Different Diet

Further analysis of the metatranscriptome of gut microbes revealed their metabolic variations across the different experimental treatments. The DEGs of gut microbiota is summarized in Table S6 (P limitation) and Table S7 (N limitation). At the KEGG module level, more up-regulated genes were found in the metabolic modules of citrate cycle, glycolysis, propanoate metabolism, and pyruvate metabolism in both N and P limitation experiment (Fig .6A). Within energy metabolism category, more up-regulated genes were found in the modules of oxidative phosphorylation and methane metabolism in both N and P limitation. Noticeably, both N and P limitation exhibited more down-regulated genes in the sulfur metabolism module.

At gene level, it is interesting to find that N and P limitation had dramatically influenced the expression pattern of nutrient metabolism related genes in the gut microbes. For example, when comparing with the Normal group, the phosphate metabolism related genes polyphosphate kinase (*PPK*), alkaline phosphatase (*phoA*), phosphate transport system (*pstS*), aspartate aminotransferase (*aspC*), and dihydrolipoamide acetyltransferase (*pdhC*) were all up-regulated in P limited diet, while all these genes were down-regulated in the N limited diet (Fig. 6B, C). As the gene encoding for glutamine synthetase (*glnA*) plays an important role in both N and P assimilation in bacteria, it was found to be up-regulated in both N- and P limited diet. In addition, the previous mentioned down-regulated genes related to sulfur metabolism in both treatments were genes encoding the anaerobic dimethyl sulfoxide reductase (*dmsC* and *dmsB*). Similarly, the anaerobic fermentation related genes (*gdhA*) were also down-regulated in both treatments (Fig. 6B, C).

The metabolic response of D. magna **under different diet**

The analysis of *D. magna* affiliated genes revealed that the nutrient limited diets mainly affect the energy produce, digestion, and cell replication related genes when compared with the nutrient replete diet. The DEGs of gut microbiota is summarized in Table S8 (P limitation) and Table S9 (N limitation). For instance, at KEGG module level, there were more DEGs enriched in cell replication category (spliceosome, Nucleotide sugar biosynthesis, RNA polymerase, DNA polymerase, and Aminoacyl-tRNA biosynthesis), energy produce category (pyruvate oxidation, F-type ATPase, and Cytochrome C oxidase), and digestion categoty (glycolysis, proteasome, and Beta-oxidation modules) (Fig. 7A). In addition, genes affiliated to the immune system of *D. magna* also showed dramatic difference across the treatments (Fig. S3). The result showed that genes affiliated to the KEGG modules, ‘defense response to the bacterium’ and ‘antimicrobial humoral response’, were significantly up-regulated in the P-limited group and down-regulated in the N-limited group, when compared with the nutrient-balanced group. In contrast, the genes involved in the ‘negative regulation of defense to the bacterium’, were up-regulated and down-regulated in N- and P-limited groups, respectively, when compared with the nutrient-balanced group.

Using CCA, the putative associations of the main differentially expressed genes among the gut microbes and *D. magna* were revealed (Fig. 6B). It is interesting to find that the expression level of gut microbes related genes encoding for phosphorus metabolism (*PPK* and *pstS*) and *D. magna* affiliated genes encoding for digestion were positive correlated in P limited diet, but the correlation turned to be negative in N limited diet. The glycolysis related microbial genes were positive correlated with the host associated genes for digestion and cell division in both N and P limited diet. In addition, the microbial expression level for the biosynthesis of the host beneficial representative short-chain fatty acid (SCFA), butyrate, was found to decrease in all nutrient-imbalanced algal diet (Fig. 6C).

Rna Sequencing Validation By Qpcr

To validate the RNA sequencing results, six microbial genes and seven *D. magna* genes that are known to be involved in important biological functions were selected for further validation via an RT-qPCR approach. The result of qPCR is consistent with the RNA sequencing data of gut microbe (Fig. S4) and *D. magna* (Fig. S5), confirming the credibility of the RNA sequencing results.

Discussion

The dynamic gut microbial community consists of ingested bacteria that pass through the intestinal tract, newly-settled ingested bacteria and the original residential bacteria. Thus, the environmental conditions can mediate the composition and function through affecting the ambient bacteria that may be ingested by zooplankton and settling in their intestine, resulting in an indirect effect on the growth and fitness of zooplankton. In this study, we demonstrated for the first time the effects of nutrient-imbalanced prey and environmental nutrient limitation on the interdependence and interplay between the zooplankton *D. magna*, and its gut microbiota. In previous studies (Brett et al. 2000, Elser et al. 2001), researchers mainly focused on the effects of P- and N-limited prey on zooplankton grazing and proliferation. Here, we further demonstrated that the intestinal microbiota not only help the *D. magna* to adapt to the nutrient-imbalanced prey, but they also absorb outstripped nutrients in response to a sudden increase of nutrients from the oligotrophic ambient water to the nutrient-enriched gut. As the nutrient-accumulated intestinal microbes were attached to the fecal pellets, it is reasonable to believe that these pellets play a more important role in oligotrophic aquatic systems than what we thought before.

Variations in the intestinal microbial community in nutrient-imbalanced algal diet

Living with a nutrient-imbalanced diet markedly altered the microbial community structure in the *D. magna* intestine. The normal group was characterized by enriched levels of *Ruminococcaceae* and *Xanthomonadaceae*. These bacterial families are widely distributed in the gut of metazoans (Reid et al. 2011, Donaldson et al. 2016), and they are especially effective at degrading a diverse range of polysaccharides and fibers in the gut of wood-feeding metazoans (Cho et al. 2010, Hooda et al. 2012). The high expression level of microbial SCFA synthesis genes we observed in the normal group is consistent with an enriched amount of *Ruminococcaceae*, since part of the bacteria species within it is

known to be a vital SCFA producer in the metazoan gut (Cho et al. 2010). As the gut microbe-related digestion of polysaccharides and synthesis of SCFA are both essential to the host (Kasubuchi et al. 2015, Ríos-Covián et al. 2016), the compensatory feeding behaviour and decreased reproduction ability of *D. magna* in the N- and P-limited groups might be due to the decreased amount of SCFA synthesis- and food digestion-related microbial taxa.

Planctomycetaceae were enriched in the gut of the N-limited group. This might be due to the effects of decreased microbial synthesis of butyrate in the gut (Fig. 7C), since it has previously been reported that *Planctomycetaceae* are more abundant in guts containing lower levels of butyrate (Zhai et al. 2019). Both the P- and N-limited groups had more *Streptococcaceae* in their gut; indeed, previous reports indicate that the presence of *Streptococcaceae* in the gut is highly associated with metabolic disorders of the host (Aran et al. 2011, Qiao et al. 2014).

As the mechanisms that control microbial community diversity become an intriguing question to ecologists, the relative importance of selective (niche-based or selective processes involve deterministic factors) and neutral processes (passive dispersal and ecological drift) have been widely quantified to reveal the driving force of community structure and succession (Chave 2004, Pan et al. 2019). In order to better understand whether *D. magna* subjectively selected the gut bacteria to benefit itself in nutrient-limiting conditions, we performed NCM to quantify the importance of neutral processes. The high R^2 value calculated by the model indicates that the neutral process is the main driving force that shapes the gut microbiome in different diets. When comparing with the Normal group, the increased R^2 and *m* value suggested a promoted importance of migration process in shaping the gut microbial community under the low-quality diets (Sloan et al. 2006, Burns et al. 2016). This result, in turn, demonstrated a decreased *D. magna* related influence and increased ambient-gut exchange related influence on its gut microbial community in nutrient depleted environments. Since zooplankton would ingest more prey under low-quality diet to compensate for their nutrient requirement (Suzuki-Ohno et al. 2012, Mandal et al. 2018), more bacteria could enter the gut. Therefore, passive dispersal of gut microbe triggered by the compensatory feeding may stimulate the migration process, which in turn reduce the importance of selection process in low-quality diets. Furthermore, in both treatments the down-regulated genes in anaerobic sulfur metabolism and fermentation in gut microbes could also be explained by the enhanced ingestion activity of host. As the increased water filtering activity can lead to the promotion of oxygen level in the zooplankton gut, the anaerobic sulfur and formation related metabolism could be strongly inhibited. However, this explanation still needs further verification through field experiments.

P-limitation stimulates the accumulation of microbial polyP in the gut of D. magna

Our results showed that the microbial pathways involved in the accumulation of polyP were markedly up-regulated in the P-limited group when compared with the normal group, and this was further verified through the detection of microbial polyP inside the fecal pellets produced by the zooplankton (Fig. 8). By comparing the concentration of microbial polyP in the algal prey-associated bacteria and in the free-living bacteria in *D. magna* culture medium, with that of the fecal pellet-associated bacteria, we confirmed that

the microbial accumulation of polyP had occurred inside *D. magna* intestine (Table S5). These results are consistent with previous reports, which demonstrated that bacteria can exhibit rapid and extensive polyP accumulation once inorganic P (Pi) is added to cells that were previously subjected to Pi starvation stress (Harold 1966, Hirota et al. 2010). Therefore, the nutrient-enriched environment of the *D. magna* gut provided the bacteria that were ingested with the algal prey, with excessive levels of Pi without competition from the prey. Since zooplankton fecal pellets are an essential source of nutrients for the aquatic ecosystem (Turner and Ferrante 1979, Urrère and Knauer 1981), our new findings suggest that microbial activity in the zooplankton gut might play a more important role than was originally thought in regulating the regeneration of nutrients in oligotrophic aquatic ecosystems.

N-limitation stimulates microbial nitrogen assimilation in the *D. magna* gut

Our results indicated an increased level of expression of microbial inorganic nitrogen assimilation-related genes in the N-limited group (Fig. 8). This suggests that the microbiota that are ingested might utilize ammonia generated by the zooplankton (Bidigare 1983, Conroy et al. 2005) to compensate for their previous nitrogen starvation in ambient water. Considering the strong competition between different microorganisms and the dilution effects of ammonia once it is excreted (Sommer 2002, Hambright et al. 2007), the intestinal bacteria seem to have a better supply of nitrogen than those living outside the gut. Since some of the ingested microbes are released into the ambient water on fecal pellets (Ploug et al. 2008, Tang et al. 2010), utilization of the *D. magna* excreted nitrogen source during their passage through the gut, might enhance their physiological fitness in nitrogen-limited environments.

Effects of nutrient limitation on the cooperation between the gut microbiota and D. magna in nutrient provision

Our sterile feeding experiment showed that when the food quality is poor, the existing gut microbiota can still benefit the *D. magna* by enhancing their growth and survival, rather than solely competing for the nutrients that are lacking. The positive correlation between host genes essential for survival (digestion and growth) and gut microbial genes for glycolysis illustrated that the gut microbe could help the host in food digestion and growing under nutrient limited condition. These results are consistent with those from previous reports, which indicate that gut microbiota are essential for the growth and survival of zooplankton under different environmental conditions (Callens et al. 2018, Li et al. 2019b). We also discovered that the expression level of antimicrobial genes in the host immune system was increased in the P-limited group. This might be explained by the massive requirement of phosphorus by zooplankton, and the potential nutrient competition between the gut microbiota and their host. For example, it has been reported that phosphorus-limited prey are more damaging toward zooplankton than are nitrogen-limited prey (Boersma 2000, Elser et al. 2001). Interestingly, although there were some host-generated negative effects on the gut microbiota in P-limited conditions, *D. magna* were still beneficial from the existing intestinal microbes. This could due to the promoted digestion and absorption capability of *D. magna* when the gut microbiota are existing (Callens et al. 2016, Callens et al. 2018). Therefore, we suggest that by entering the gut of *D. magna*, bacteria not only benefit themselves by absorbing more nutrients inside

the gut of their host, but also benefit the host by improving their growth in a nutrient-imbalanced algal diet.

Conclusion

In summary, metatranscriptomic study of the effects of nutrient-imblanced algal diet on the metabolism and community composition of *D. magna*'s gut microbiota revealed that P and N limited prey promoted polyP accumulation and nitrogen assimilation in the gut microbiota, respectively. The NCM results suggested that under nutrient-limiting conditions the influence of the host in selecting the gut microbial community was reduced, while the passive dispersal processes were promoted possibly through the compensatory feeding. A nearly axenic grazing experiment demonstrated that the microbiota inside the gut of *D. magna* was not only benefited from the nutrient rich gut environment, but they also helped *D. magna* to achieve better growth in low-quality diet. Altogether, our study, for the first time, revealed that there is an increased chance for ambient bacteria to enter *D. magna*'s gut under nutrient limited conditions, and these ingested bacteria can absorb excess nutrients and benefit the growth of their zooplankton host at the same time.

Declarations

Data availability statement

Sequence data was deposited in GenBank (Sequence Read Archive) and is available under the BioProject PRJNA597965.

Acknowledgements

This study was supported by the Hong Kong Branch of Southern Marine Science and Engineering Guangdong Laboratory (Guangzhou) (SMSEGL20SC01).

Competing Interests

The authors declare that there is no conflict of interest.

References

1. Aran A, Lin L, Finn LA, Weiner K, Peppard P, Young T, Mignot E. Post-streptococcal antibodies are associated with metabolic syndrome in a population-based cohort. PloS one. 2011;6:e25017.
2. Bidigare RR. 1983. Nitrogen excretion by marine zooplankton. Nitrogen in the marine environment:385–409.
3. Binks PR, French CE, Nicklin S, Bruce NC. Degradation of pentaerythritol tetranitrate by Enterobacter cloacae PB2. Appl Environ Microbiol. 1996;62:1214–9.

4. Boersma M. The nutritional quality of P-limited algae for Daphnia. Limnol Oceanogr. 2000;45:1157–61.
5. Boersma M, Aberle N, Hantzsche FM, Schoo KL, Wiltshire KH, Malzahn AM. Nutritional limitation travels up the food chain. Int Rev Hydrobiol. 2008;93:479–88.
6. Brett MT, Müller-Navarra DC, Sang-Kyu P. Empirical analysis of the effect of phosphorus limitation on algal food quality for freshwater zooplankton. Limnol Oceanogr. 2000;45:1564–75.
7. Brune A, Dietrich C. The gut microbiota of termites: digesting the diversity in the light of ecology and evolution. Annu Rev Microbiol. 2015;69:145–66.
8. Buchfink B, Xie C, Huson DH. Fast and sensitive protein alignment using DIAMOND. Nature methods. 2015;12:59.
9. Burns AR, Stephens WZ, Stagaman K, Wong S, Rawls JF, Guillemin K, Bohannan BJ. Contribution of neutral processes to the assembly of gut microbial communities in the zebrafish over host development. ISME J. 2016;10:655–64.
10. Callens M, Macke E, Muylaert K, Bossier P, Lievens B, Waud M, Decaestecker E. Food availability affects the strength of mutualistic host–microbiota interactions in Daphnia magna. ISME J. 2016;10:911–20.
11. Callens M, Watanabe H, Kato Y, Miura J, Decaestecker E. Microbiota inoculum composition affects holobiont assembly and host growth in Daphnia. Microbiome. 2018;6:56.
12. Camacho C, Coulouris G, Avagyan V, Ma N, Papadopoulos J, Bealer K, Madden TL. BLAST+: architecture and applications. BMC Bioinform. 2009;10:421.
13. Carlson CA, Hansell DA. 2015. DOM sources, sinks, reactivity, and budgets. Pages 65–126 Biogeochemistry of marine dissolved organic matter. Elsevier.
14. Chave J. Neutral theory and community ecology. Ecology letters. 2004;7:241–53.
15. Chen W, Pan Y, Yu L, Yang J, Zhang W. Patterns and processes in marine microeukaryotic community biogeography from Xiamen coastal waters and intertidal sediments, southeast China. Frontiers in microbiology. 2017;8:1912.
16. Chevalier C, Stojanović O, Colin DJ, Suarez-Zamorano N, Tarallo V, Veyrat-Durebex C, Rigo D, Fabbiano S, Stevanović A, Hagemann S. Gut microbiota orchestrates energy homeostasis during cold. Cell. 2015;163:1360–74.
17. Cho M-J, Kim Y-H, Shin K, Kim Y-K, Kim Y-S, Kim T-J. Symbiotic adaptation of bacteria in the gut of Reticulitermes speratus: Low endo-β-1, 4-glucanase activity. Biochem Biophys Res Commun. 2010;395:432–5.
18. Conroy JD, Edwards WJ, Pontius RA, Kane DD, Zhang H, Shea JF, Richey JN, Culver DA. Soluble nitrogen and phosphorus excretion of exotic freshwater mussels (Dreissena spp.): potential impacts for nutrient remineralisation in western Lake Erie. Freshw Biol. 2005;50:1146–62.
19. Donaldson GP, Lee SM, Mazmanian SK. Gut biogeography of the bacterial microbiota. Nat Rev Microbiol. 2016;14:20–32.

20. Edgar RC, Haas BJ, Clemente JC, Quince C, Knight R. UCHIME improves sensitivity and speed of chimera detection. Bioinformatics. 2011;27:2194–200.
21. Elser JJ, Hayakawa K, Urabe J. Nutrient limitation reduces food quality for zooplankton: Daphnia response to seston phosphorus enrichment. Ecology. 2001;82:898–903.
22. Elser JJ, Urabe J. The stoichiometry of consumer-driven nutrient recycling: theory, observations, and consequences. Ecology. 1999;80:735–51.
23. Foster JA, Neufeld K-AM. Gut–brain axis: how the microbiome influences anxiety and depression. Trends in neurosciences. 2013;36:305–12.
24. Glibert PM, Fullerton D, Burkholder JM, Cornwell JC, Kana TM. Ecological stoichiometry, biogeochemical cycling, invasive species, and aquatic food webs: San Francisco Estuary and comparative systems. Rev Fish Sci. 2011;19:358–417.
25. Golz A-L, Burian A, Winder M. Stoichiometric regulation in micro-and mesozooplankton. J Plankton Res. 2015;37:293–305.
26. Gong W, Paerl H, Marchetti A. Eukaryotic phytoplankton community spatiotemporal dynamics as identified through gene expression within a eutrophic estuary. Environ Microbiol. 2018;20:1095–111.
27. Grasshoff K, Kremling K, Ehrhardt M. 2009. Methods of seawater analysis. John Wiley & Sons.
28. Haas BJ, Papanicolaou A, Yassour M, Grabherr M, Blood PD, Bowden J, Couger MB, Eccles D, Li B, Lieber M. De novo transcript sequence reconstruction from RNA-seq using the Trinity platform for reference generation and analysis. Nature protocols. 2013;8:1494.
29. Hambright K, Hairston N, Schaffner W, Howarth R. Grazer control of nitrogen fixation: synergisms in the feeding ecology of two freshwater crustaceans. Fundamental Applied Limnology/Archiv für Hydrobiologie. 2007;170:89–101.
30. Harold FM. Inorganic polyphosphates in biology: structure, metabolism, and function. Bacteriological Reviews. 1966;30:772.
31. Hessen DO, Ågren GI, Anderson TR, Elser JJ. and P. C. De Ruiter. 2004. Carbon sequestration in ecosystems: the role of stoichiometry. Ecology **85**:1179–1192.
32. Hirota R, Kuroda A, Kato J, Ohtake H. Bacterial phosphate metabolism and its application to phosphorus recovery and industrial bioprocesses. Journal of bioscience bioengineering. 2010;109:423–32.
33. Hooda S, Boler BMV, Serao MCR, Brulc JM, Staeger MA, Boileau TW, Dowd SE, Fahey GC Jr, Swanson KS. 454 pyrosequencing reveals a shift in fecal microbiota of healthy adult men consuming polydextrose or soluble corn fiber. J Nutr. 2012;142:1259–65.
34. AND FUNGAL CONTAMINATION IN THE GREEN ALGA CHLAMYDOMONAS REINHARDTII CULTURE BY USING AN ANTIBIOTIC COCKTAIL 1
Kan Y, Pan J. 2010. A ONE-SHOT SOLUTION TO BACTERIAL. AND FUNGAL CONTAMINATION IN THE GREEN ALGA CHLAMYDOMONAS REINHARDTII CULTURE BY USING AN ANTIBIOTIC COCKTAIL 1. Journal of phycology **46**:1356–1358.

35. Kasubuchi M, Hasegawa S, Hiramatsu T, Ichimura A, Kimura I. Dietary gut microbial metabolites, short-chain fatty acids, and host metabolic regulation. Nutrients. 2015;7:2839–49.
36. Klüttgen B, Dülmer U, Engels M, Ratte H. ADaM, an artificial freshwater for the culture of zooplankton. Water Res. 1994;28:743–6.
37. Kulakova AN, Hobbs D, Smithen M, Pavlov E, Gilbert JA, Quinn JP, McGrath JW. Direct quantification of inorganic polyphosphate in microbial cells using 4'-6-diamidino-2-phenylindole (DAPI). Environ Sci Technol. 2011;45:7799–803.
38. Langmead B, Salzberg SL. Fast gapped-read alignment with Bowtie 2. Nature methods. 2012;9:357.
39. Leitão-Gonçalves R, Carvalho-Santos Z, Francisco AP, Fioreze GT, Anjos M, Baltazar C, Elias AP, Itskov PM, Piper MD, Ribeiro C. Commensal bacteria and essential amino acids control food choice behavior and reproduction. PLoS Biol. 2017;15:e2000862.
40. Li H, Handsaker B, Wysoker A, Fennell T, Ruan J, Homer N, Marth G, Abecasis G, Durbin R. The sequence alignment/map format and SAMtools. Bioinformatics. 2009;25:2078–9.
41. Li Y, Jing H, Xia X, Cheung S, Suzuki K, Liu H. Metagenomic insights into the microbial community and nutrient cycling in the western subarctic pacific ocean. Front Microbiol. 2018;9:623.
42. Li Y, Neng Y, Wong TY, Wang W-X, Liu H. 2019a. Interaction of antibacterial silver nanoparticles and microbiota-dependent holobiont revealed by metatranscriptomic analysis. Environmental Science: Nano.
43. Li Y, Yan N, Wong TY, Wang W-X, Liu H. Interaction of antibacterial silver nanoparticles and microbiota-dependent holobionts revealed by metatranscriptomic analysis. Environmental Science: Nano. 2019b;6:3242–55.
44. Liu H, Tan S, Xu J, Guo W, Xia X, Yan Cheung S. Interactive regulations by viruses and dissolved organic matter on the bacterial community. Limnol Oceanogr. 2017;62:364–80.
45. Macke E, Callens M, De Meester L, Decaestecker E. Host-genotype dependent gut microbiota drives zooplankton tolerance to toxic cyanobacteria. Nature communications. 2017a;8:1608.
46. Macke E, Callens M, Meester L, Decaestecker E. Host-genotype dependent gut microbiota drives zooplankton tolerance to toxic cyanobacteria. Nature communications. 2017b;8:1608.
47. Mandal S, Abbott Wilkins R, Shurin JB. Compensatory grazing by Daphnia generates a trade-off between top-down and bottom-up effects across phytoplankton taxa. Ecosphere. 2018;9:e02537.
48. Marchet C, Lecompte L, Limasset A, Bittner L, Peterlongo P. 2018. A resource-frugal probabilistic dictionary and applications in bioinformatics. Discrete Applied Mathematics.
49. Marie D, Partensky F, Jacquet S, Vaulot D. Enumeration and cell cycle analysis of natural populations of marine picoplankton by flow cytometry using the nucleic acid stain SYBR Green I. Appl Environ Microbiol. 1997;63:186–93.
50. Meng A, Marchet C, Corre E, Peterlongo P, Alberti A, Da Silva C, Wincker P, Pelletier E, Probert I, Decelle J. A de novo approach to disentangle partner identity and function in holobiont systems. Microbiome. 2018;6:105.

51. Orsini L, Gilbert D, Podicheti R, Jansen M, Brown JB, Solari OS, Spanier KI, Colbourne JK, Rusch DB, Decaestecker E. Daphnia magna transcriptome by RNA-Seq across 12 environmental stressors. Scientific data. 2016;3:160030.
52. Pan Y, Yang J, McManus GB, Lin S, Zhang W. 2019. Insights into protist diversity and biogeography in intertidal sediments sampled across a range of spatial scales. Limnology and Oceanography.
53. Pearson WR, Wood T, Zhang Z, Miller W. Comparison of DNA sequences with protein sequences. Genomics. 1997;46:24–36.
54. Ploug H, Iversen MH, Fischer G. Ballast, sinking velocity, and apparent diffusivity within marine snow and zooplankton fecal pellets: Implications for substrate turnover by attached bacteria. Limnol Oceanogr. 2008;53:1878–86.
55. Prahl FG, Carpenter R. The role of zooplankton fecal pellets in the sedimentation of polycyclic aromatic hydrocarbons in Dabob Bay. Washington Geochimica et Cosmochimica Acta. 1979;43:1959–72.
56. Qiao Y, Sun J, Xie Z, Shi Y, Le G. Propensity to high-fat diet-induced obesity in mice is associated with the indigenous opportunistic bacteria on the interior of Peyer's patches. Journal of clinical biochemistry nutrition. 2014;55:120–8.
57. Reid NM, Addison SL, Macdonald LJ, Lloyd-Jones G. Biodiversity of active and inactive bacteria in the gut flora of wood-feeding huhu beetle larvae (Prionoplus reticularis). Appl Environ Microbiol. 2011;77:7000–6.
58. Ríos-Covián D, Ruas-Madiedo P, Margolles A, Gueimonde M, C. G. de los Reyes-Gavilán, and N. Salazar. 2016. Intestinal short chain fatty acids and their link with diet and human health. Frontiers in microbiology **7**:185.
59. Rippka R, Deruelles J, Waterbury JB, Herdman M, Stanier RY. Generic assignments, strain histories and properties of pure cultures of cyanobacteria. Microbiology. 1979;111:1–61.
60. Robertson G, Schein J, Chiu R, Corbett R, Field M, Jackman SD, Mungall K, Lee S, Okada HM, Qian JQ. De novo assembly and analysis of RNA-seq data. Nature methods. 2010;7:909–12.
61. Robinson MD, McCarthy DJ, Smyth GK. edgeR: a Bioconductor package for differential expression analysis of digital gene expression data. Bioinformatics. 2010;26:139–40.
62. Sloan WT, Lunn M, Woodcock S, Head IM, Nee S, Curtis TP. Quantifying the roles of immigration and chance in shaping prokaryote community structure. Environ Microbiol. 2006;8:732–40.
63. Sommer U. 2002. Competition and coexistence in plankton communities. Pages 79–108 Competition and coexistence. Springer.
64. Steinberg DK, Landry MR. Zooplankton and the ocean carbon cycle. Annual Review of Marine Science. 2017;9:413–44.
65. Sterner RW, Clasen J, Lampert W, Weisse T. Carbon: phosphorus stoichiometry and food chain production. Ecol Lett. 1998;1:146–50.

66. Sterner RW, Elser JJ. 2002. Ecological stoichiometry: the biology of elements from molecules to the biosphere. Princeton university press.
67. Suzuki-Ohno Y, Kawata M, Urabe J. Optimal feeding under stoichiometric constraints: a model of compensatory feeding with functional response. Oikos. 2012;121:569–78.
68. Tang KW, Turk V, Grossart H-P. Linkage between crustacean zooplankton and aquatic bacteria. Aquat Microb Ecol. 2010;61:261–77.
69. Turner JT, Ferrante JG. Zooplankton fecal pellets in aquatic ecosystems. Bioscience. 1979;29:670–7.
70. Urrère MA, Knauer GA. Zooplankton fecal pellet fluxes and vertical transport of particulate organic material in the pelagic environment. J Plankton Res. 1981;3:369–87.
71. Vital M, Howe AC, Tiedje JM. Revealing the bacterial butyrate synthesis pathways by analyzing (meta) genomic data. MBio. 2014;5:e00889-00814.
72. Xu J, Jing H, Kong L, Sun M, Harrison PJ, Liu H. Effect of seawater–sewage cross-transplants on bacterial metabolism and diversity. Microbial ecology. 2013;66:60–72.
73. Zhai S, Qin S, Li L, Zhu L, Zou Z, Wang L. Dietary butyrate suppresses inflammation through modulating gut microbiota in high-fat diet-fed mice. FEMS Microbiol Lett. 2019;366:fnz153.
74. Zhang S, Liu H, Chen B, Wu C-J. Effects of diet nutritional quality on the growth and grazing of Noctiluca scintillans. Mar Ecol Prog Ser. 2015;527:73–85.
75. Zhang S, Liu H, Glibert PM, Guo C, Ke Y. Effects of prey of different nutrient quality on elemental nutrient budgets in Noctiluca scintillans. Scientific reports. 2017;7:7622.
76. Xu J, Ho AY, Yin K, Yuan X, Anderson DM, Lee JH, Harrison PJ. Temporal and spatial variations in nutrient stoichiometry and regulation of phytoplankton biomass in Hong Kong waters: influence of the Pearl River outflow and sewage inputs. Mar Pollut Bull. 2008;57:335–48.

Figures

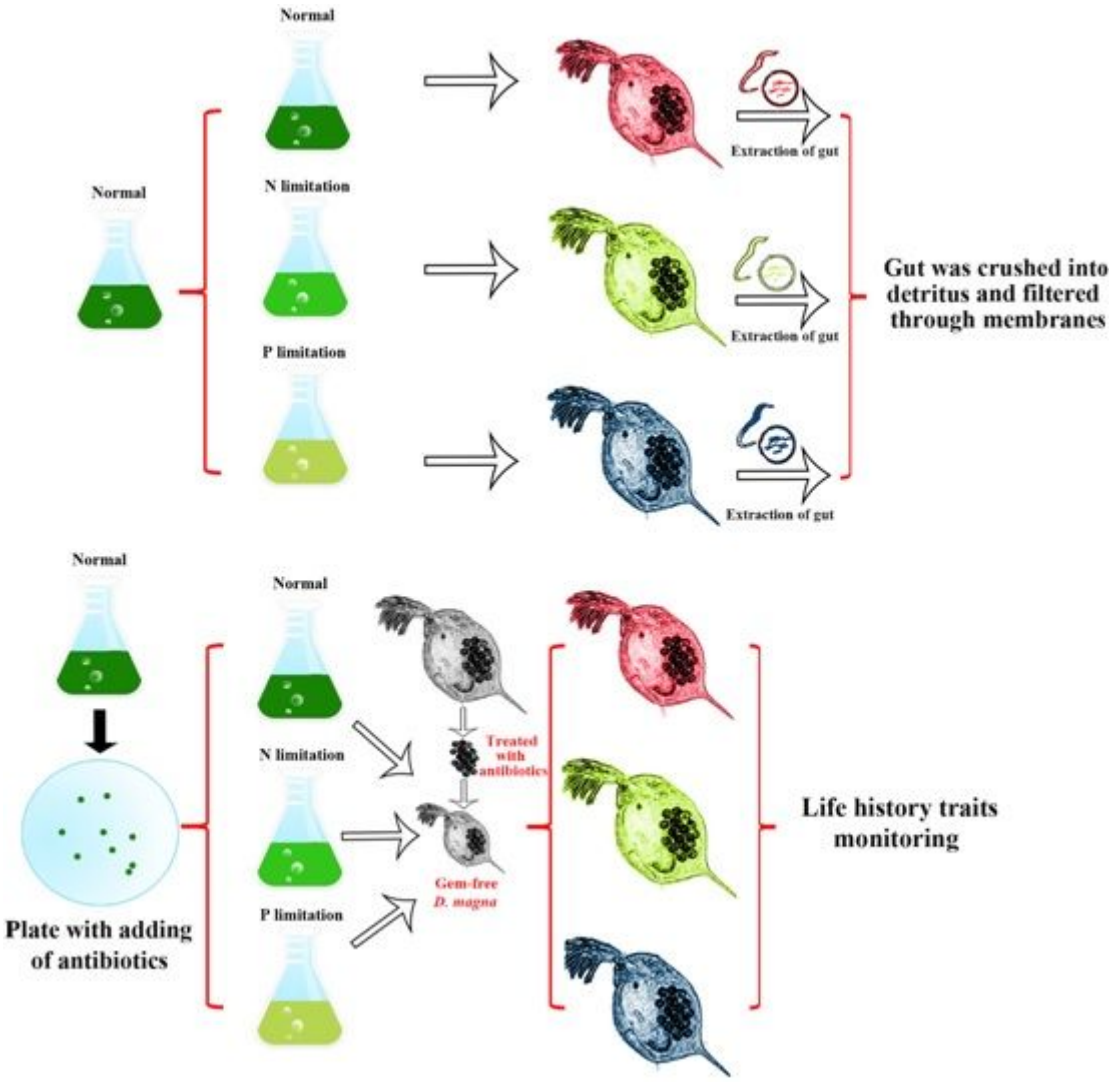

Figure 1

Schematic diagram showing the experimental procedure

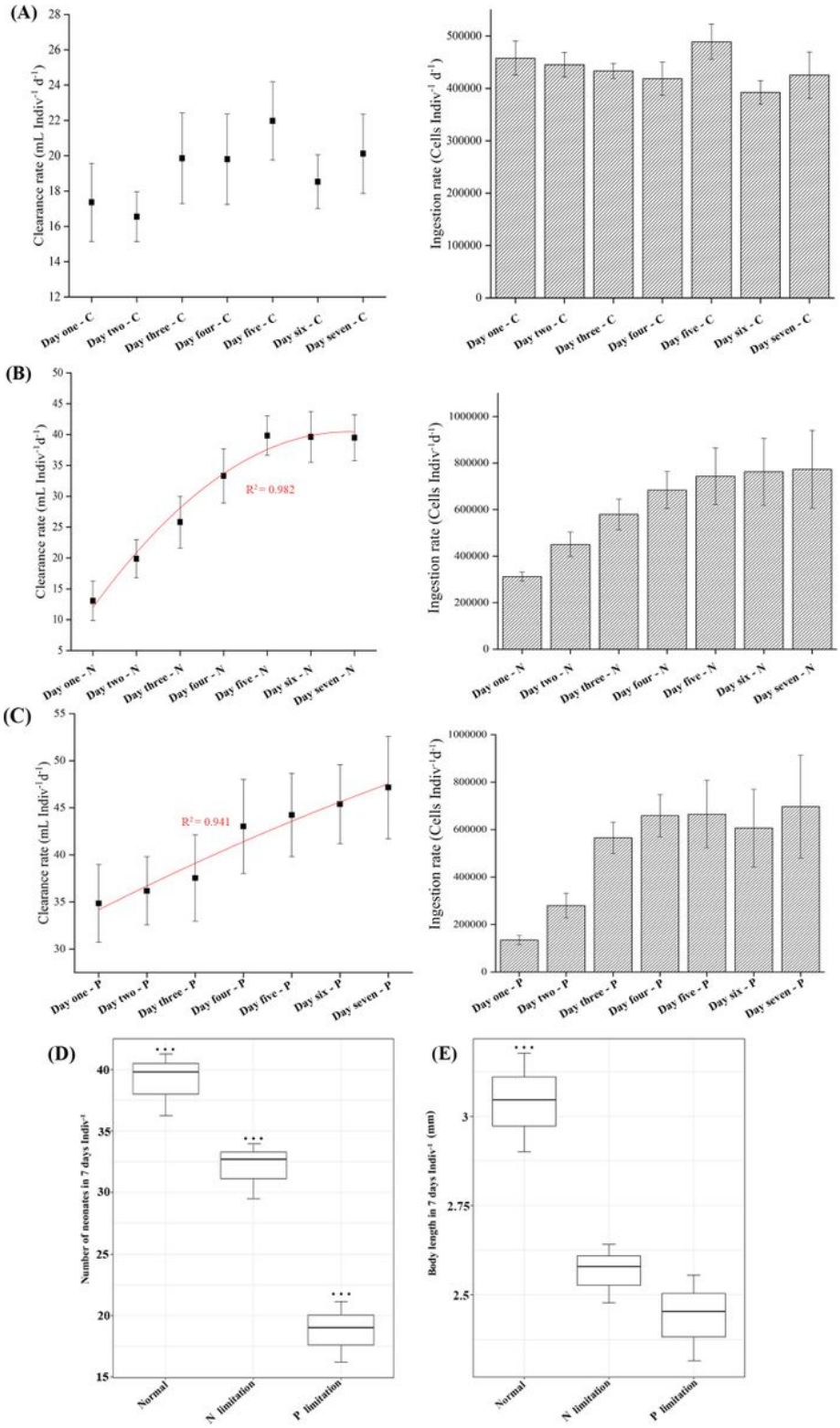

Figure 2

(A) D. magna related clearance and ingestion rate during 7 days under nutrient balanced condition. The clearance and ingestion rate of D. magna during 7 days under (B) N- and (C) P-limitation. (D) The number of neonates generated by each D. magna over a period of 7 days, and (E) the body length of D. magna at the end of 7 days following the different experimental treatments shown.

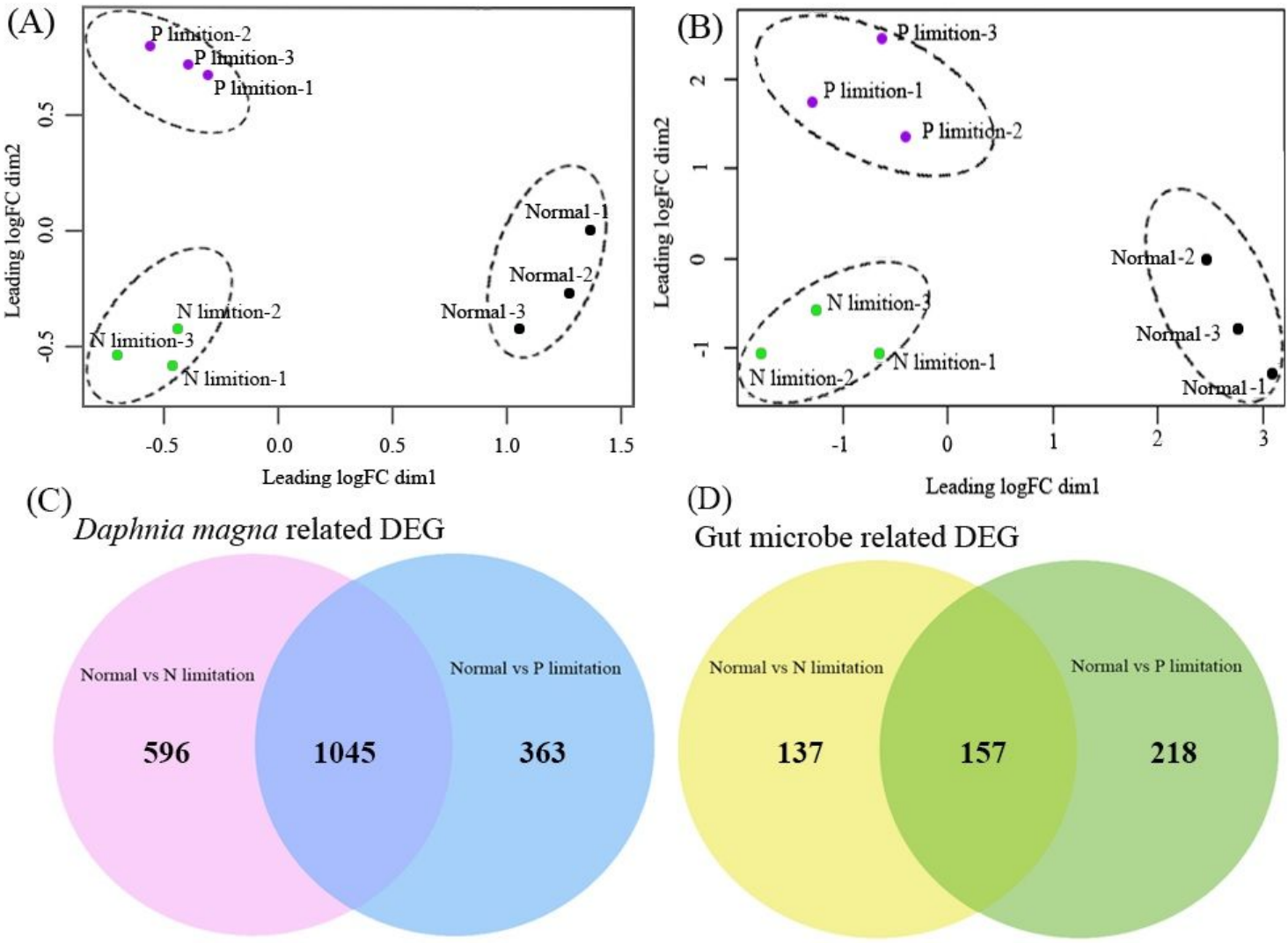

Figure 3

Principal component analysis of transcriptomic data affiliated to host (A) and gut microbiota (B), using normalized gene expression counts for each experimental group. Venn diagrams showing the differential expression genes (DEGs) among the different treatment groups for (C) D. magna and (D) gut microbiota.

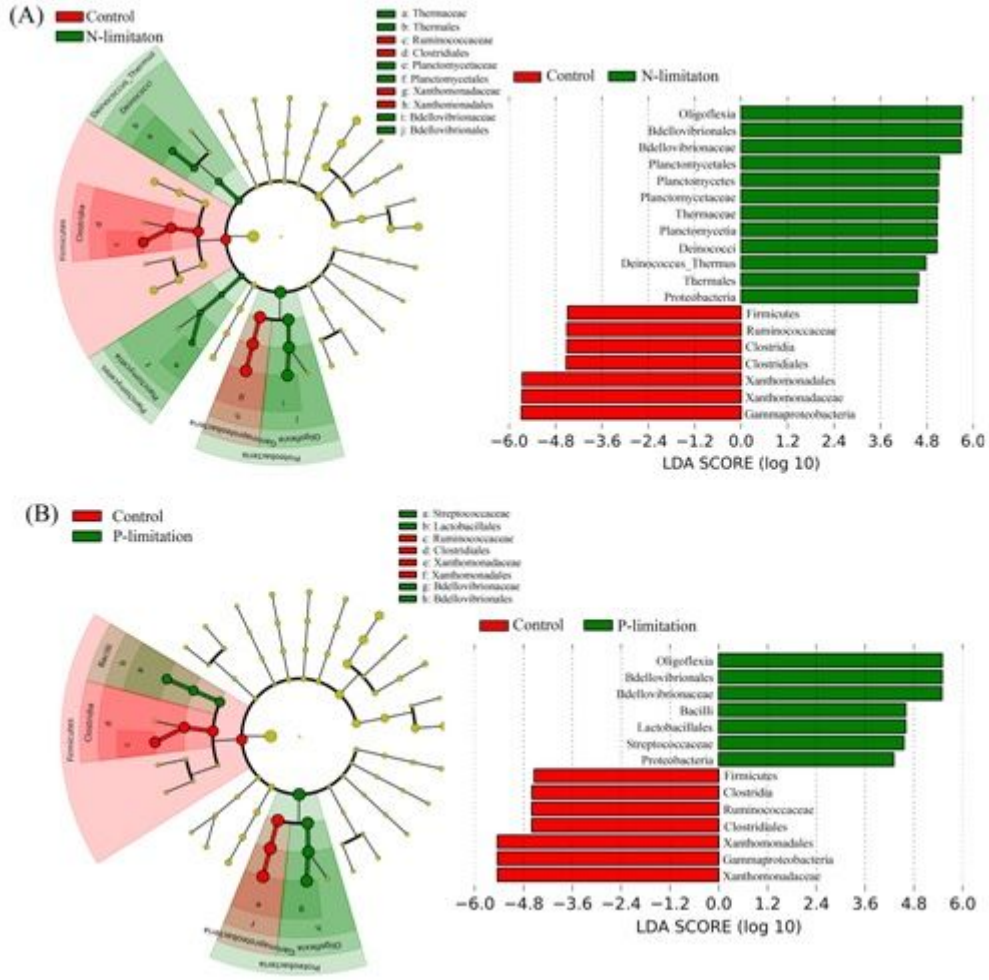

Figure 4

Cladogram indicating the phylogenetic distribution of the microbial lineages in the different experimental treatment groups. The LDA score of the taxa representing the odds of their distribution among the comparison of control versus N limitation (A) and control versus P limitation (B).

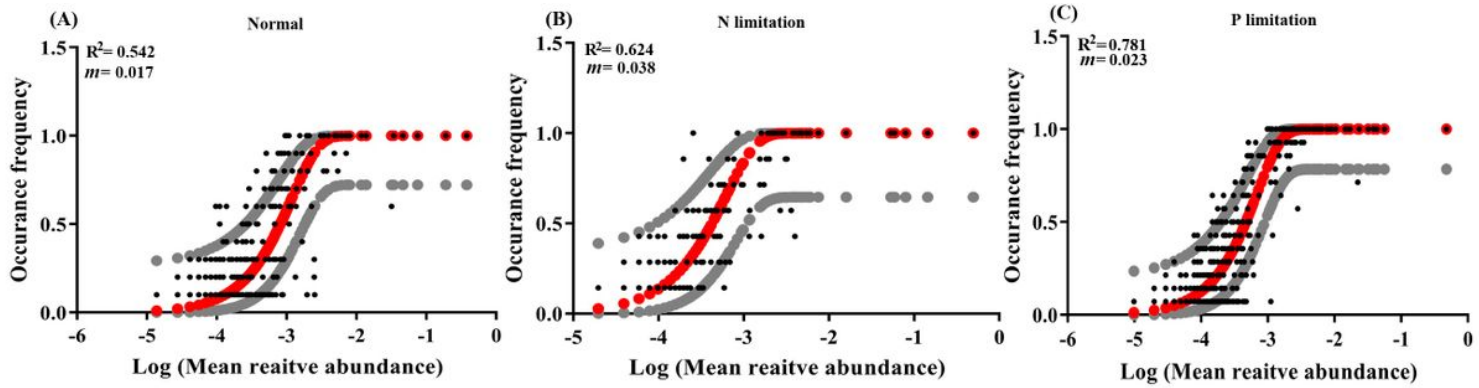

Figure 5

Fit of the neutral model for gut microbial community. (A) Gut microbial community in the Normal experimental group. (B) Gut microbial community in the N limitation experimental group. (C) Gut microbial community in the P limitation experimental group. Grey lines represent 95% confidence intervals around the model prediction (solid black line). R2 indicates the fit to the neutral model, and m indicates the immigration rate.

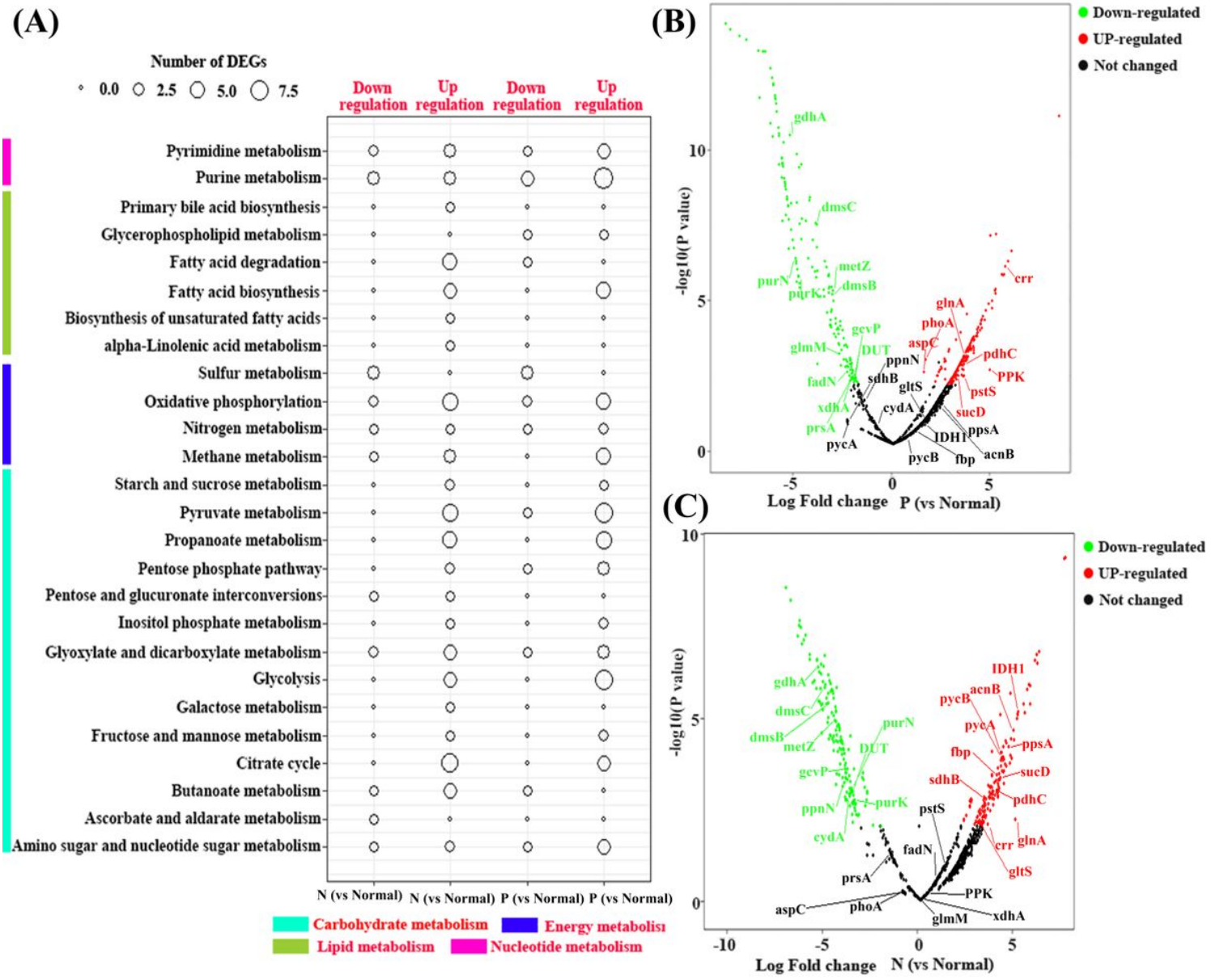

Figure 6

(A) The differentially expressed genes (DEGs) of gut microbiota within different comparison groups at the KEGG module level. (B) DEGs of gut microbiota at gene level in P limited diet (B) and N limited diet (C) with important items highlighted. acnB (K01682): aconitate hydratase 2 / 2-methylisocitrate dehydratase; aspC (K00813): aspartate aminotransferase; crr (K02777): PTS system, glucose-specific IIA component; cydA (K00425): cytochrome d ubiquinol oxidase subunit I; dmsB (K00184): dimethyl sulfoxide reductase iron-sulfur subunit; dmsC (K00185): dimethyl sulfoxide reductase membrane subunit; DUT (K01520): dUTP pyrophosphatase; fadN (K07516): 3-hydroxyacyl-CoA dehydrogenase; fbp (K03841): fructose-1,6-

bisphosphatase I; gcvP (K00281): glycine dehydrogenase; gdhA (K00261): glutamate dehydrogenase (NAD(P)+); glmM (K03431): phosphoglucosamine mutase; glnA (K01915): glutamine synthetase; gltS (K00284): glutamate synthase (ferredoxin); IDH1(K00031): isocitrate dehydrogenase; metZ (K10764): O-succinylhomoserine sulfhydrylase; pdhC (K00627): pyruvate dehydrogenase E2 component (dihydrolipoamide acetyltransferase); phoA (K01077): alkaline phosphatase; PPK (K00937): polyphosphate kinase; ppnN (K06966): uncharacterized protein; ppsA (K01007): pyruvate, water dikinase; prsA (K00948): ribose-phosphate pyrophosphokinase; pstS (K02040): phosphate transport system substrate-binding protein; purK (K01589): 5-(carboxyamino)imidazole ribonucleotide synthase; purN (K11175): phosphoribosylglycinamide formyltransferase 1; pycA (K01959): pyruvate carboxylase subunit A; pycB (K01960): pyruvate carboxylase subunit B; sdhB (K00240): succinate dehydrogenase / fumarate reductase, iron-sulfur subunit; sucD (K01902): succinyl-CoA synthetase alpha subunit; xdhA (K13481): xanthine dehydrogenase small subunit.

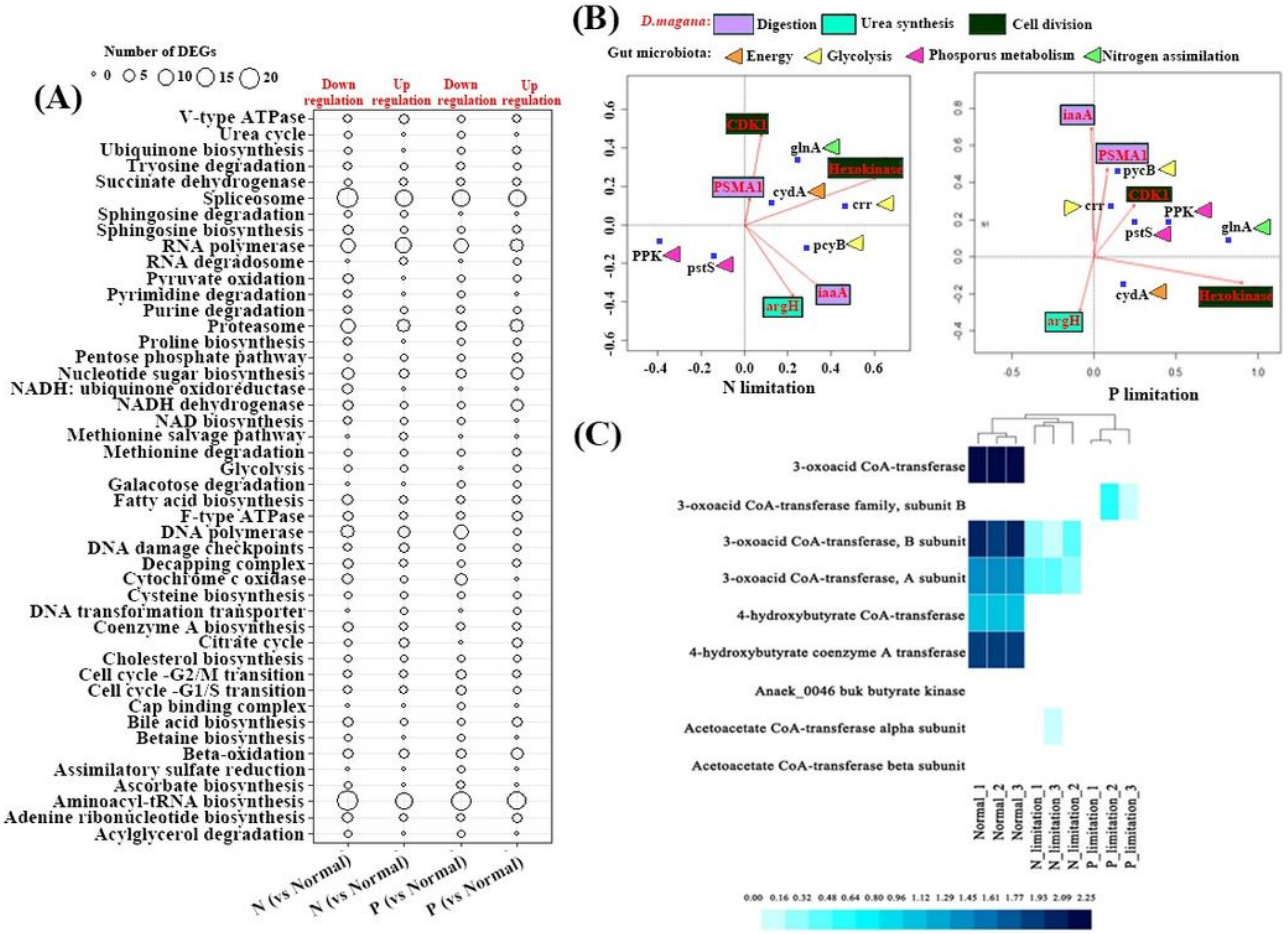

Figure 7

(A) Differentially expressed genes in the D. magna among different experimental groups at module level. (B) Canonical correlation analysis (CCA) of the expression level of essential genes between D. magna and its gut microbiota. (C) Expression level of microbial genes involved in butyrate synthesis among the different experimental groups.

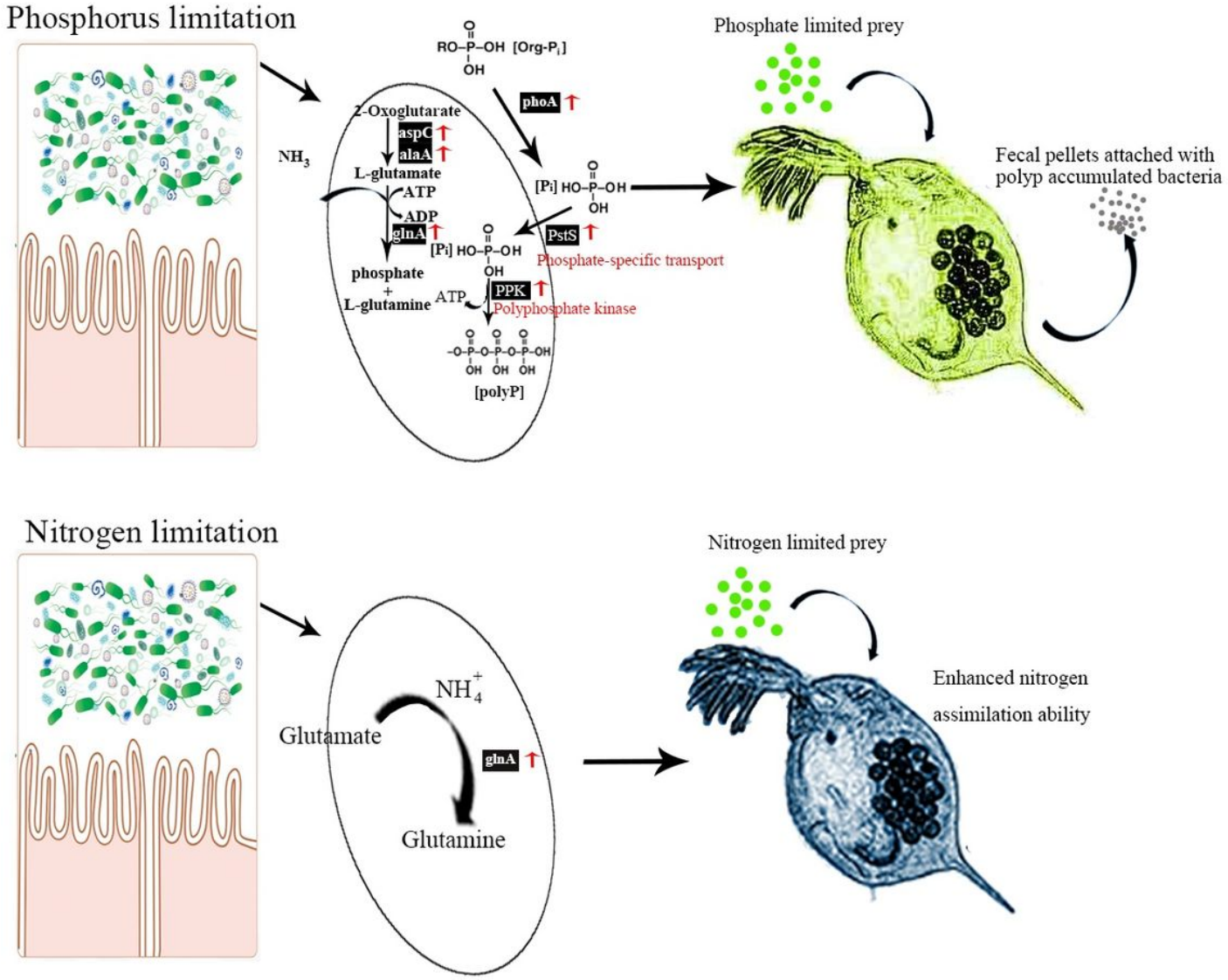

Figure 8

Schematic representation of the main biological pathways in the gut microbiota affected by low quality food. Ingestion of phosphorus-limited prey led to a stimulated accumulation of microbial polyP in the zooplankton gut, whereas ingestion of nitrogen-limited prey promoted nitrogen assimilation metabolism in the intestinal microbiota.

Supplementary Files

This is a list of supplementary files associated with this preprint. Click to download.

- Supplymentarymaterial.doc